JOURNAL OF MAPS, 2017
VOL. 13, NO. 2, 438–448
https://doi.org/10.1080/17445647.2017.1302364

SCIENCE

OPEN ACCESS Check for updates

Anisotropy of magnetic susceptibility of the Pyrenean granites

Manuel Porquet [a,b], Emilio L. Pueyo[a,c], Teresa Román-Berdiel[c,d], Philippe Olivier[e], Luis A. Longares[b], Julia Cuevas[f], Javier Ramajo[c,d] and the Geokin3DPyr working group by alphabetical order; Borja Antolín[c,d], Aitor Aranguren[f], Jean Baptiste Auréjac[e], Jean-Luc Bouchez[e], Antonio M. Casas[c,d], Yoann Denèle[e], Gerard Gleizes[e], Asier Hilario[f], Esther Izquierdo-Llavall[c,d], Dennis Leblanc[e], Belén Oliva-Urcia[c,d], Vicente Santana[f], José M. Tubía[f], Nestor Vegas[f]

[a]Instituto Geológico y Minero de España (IGME) – Unidad de Zaragoza, Zaragoza, Spain; [b]Departamento de Geografía y Ordenación del Territorio, Universidad de Zaragoza, Zaragoza, Spain; [c]Unidad Asociada en Ciencias de la Tierra IGME/Universidad de Zaragoza, Universidad de Zaragoza, Zaragoza, Spain; [d]Departamento de Ciencias de la Tierra, Universidad de Zaragoza, Zaragoza, Spain; [e]GET–UMR 5563, Université de Toulouse, CNRS, IRD, OMP, Toulouse, France; [f]Departamento de Geodinámica, Universidad del Pais Vasco / EHU, Bilbao, Spain.

ABSTRACT

In this paper, we report on a compilation of more than 2200 sites (more than 10,000 individual measurements) where anisotropy of magnetic susceptibility (AMS) was studied in granites from the Variscan Pyrenees. The standardization and homogenization of this information has allowed us to produce three Main Maps that synthesize all the information related with the AMS of the Pyrenean granites. We also describe the problems found during the construction of the database (variable geo-positioning, different published information, etc.). The information derived from 21 granite bodies, the database, and the synthesis maps (magnetic susceptibility, Km, and the orientation of the magnetic foliation, plane perpendicular to k3, and of the magnetic lineation, k1) allow us to see for the first time a complete image of this important kinematic and petrographic indicator.

ARTICLE HISTORY
Received 26 May 2016
Revised 13 February 2017
Accepted 1 March 2017

KEYWORDS
AMS; Variscan Pyrenees; magnetic lineation; magnetic foliation; bulk susceptibility; granitoid

1. Introduction

Anisotropy of magnetic susceptibility (AMS) is a sound and proven technique to determine the mineral-preferred orientation of rock volumes (Borradaile & Henry, 1997; Graham, 1954; Parés, 2015; Tarling & Hrouda, 1993). It is founded on the parallelism between the crystallographic and magnetic fabrics of some paramagnetic minerals, especially phyllosilicates (Martín-Hernández & Hirt, 2003). As long as some conditions are met, AMS is a quick, inexpensive, effective, and non-destructive way to determine rock fabric, and is able to obtain the mineral-preferred orientation in rocks with apparently absent macroscopic and even microscopic evidence.

Compared to measurements on sedimentary and metamorphic rocks (Graham, 1954), the application to granite started later (Heller, 1973; King, 1966). AMS in granite with a calc-alkaline affinity seems to display a better characterization of the rock fabric when compared to classic techniques such as those based on outcrop or microscope measurements of feldspar and biotite crystals, and so on. The reason lies in the total content in iron and its mineral fractioning, a fact that promoted a classification of granites as either magnetic or non-magnetic (Ellwood & Wenner, 1981; Ishihara, 1977). For all these reasons, the application of AMS in calc-alkaline plutons (non-magnetic; iron is fractioned mostly in biotite) has represented a turning point in the interpretation of the kinematics of their emplacement modes (Bouchez, 1997). Apart from being able to precisely determine the preferred orientation of biotites in apparently isotropic rocks (a main marker of the rock fabric), AMS also yields a control of the deformation intensity (relative differences among the AMS ellipsoids) and can be used as a petrological mapping variable, being correlated with iron content (Gleizes, Nédélec, Bouchez, Autran, & Rochette, 1993).

The Geokin3Dpyr group (Communauté de Travail des Pyrénées; INTERREG III program) was formed in 2003 and integrated all Pyrenean universities and research centers in Earth Sciences. A main goal of this program was the development of electronic and public databases including the preliminary compilation of AMS data (López, Oliván, Oliva, & Pueyo, 2008; Pueyo et al., 2006). Recently, the AMS database of the Pyrenees has been completed and updated both in sedimentary rocks (Pocovi et al., 2014) and granites (Porquet, 2014). In this paper, we introduce the maps that synthesize information from the latter, where AMS data from 21 different granites and one gneissic dome (Aston) have been homogenized and compiled.

CONTACT Manuel Porquet mppardina@gmail.com; unaim@igme.es Instituto Geológico y Minero de España (IGME) – Unidad de Zaragoza, Manuel Lasala 44, 50006 Zaragoza, Spain
Supplemental data for this article can be accessed https://doi.org/10.1080/17445647.2017.1302364.

The final goal of this database is to be integrated, in the near future, in the Information Web Resources of the Geological Surveys of Spain and France (www.igme.es and www.brgm.fr, respectively).

2. Map specifications

The maps included in this paper use the ETRS 1989 datum and the UTM Zone 30 projected coordinated systems, although the eastern part of the map belongs to the 31T zone, it has been converted to 30T coordinates. All three maps fulfill the Mapping Standards of Aragón (Spain; http://idearagon.aragon.es/nca/).

The geologic map used as a background (Barnolas et al., 2008) is large scale (1:400,000) but displays enough structural features (fold axes, thrust traces, etc.). However, cartographic detail on rock ages and lithologies has been simplified considerably, following the style of Choukroune and Seguret's classic structural map (1973) of the Pyrenees.

3. Geological setting

The Pyrenees are a collision chain formed during the Late Cretaceous and Eocene epochs, up to the Miocene on the southern part of the range, due to convergence between the Iberian and Eurasian plates (Muñoz, 1992). They are located between the Gulf of Lion in the Mediterranean Sea and the Biscay Bay in the Atlantic Ocean (Muñoz, 1992; Vera, 2004). The Axial Zone of the Pyrenees (backbone of the chain), where most of the Hercynian bodies are located, depicts an antiformal geometry. It is made up of Precambrian and Paleozoic rocks affected by the Hercynian tectonic phases, reworked, to some extent, by Alpine deformations.

The Pyrenean Hercynian basement belongs to the southern part of the European Variscides (inset Figure 1), an orogenic belt mostly formed during Late Carboniferous times and partly reworked during the Alpine orogeny, and is composed of sedimentary, metamorphic, and igneous rocks, ranging in age from Upper Proterozoic to Permian epoch. The Alpine orogeny brought about an antiformal stack of basement nappes, and the subsequent exhumation of Paleozoic units in the core of the Pyrenean range during Eocene and Miocene times (Beamud et al., 2011; Fitzgerald, Muñoz, Coney, & Baldwin, 1999) allowed access to the actual outcrop, making observations of the Hercynian crust possible. Reactivation of previous Variscan structures constitutes an important deformation mechanism in Alpine tectonics, and precludes the accurate chronological and kinematic analysis of tectonic phases related to the first orogenic event.

The Variscan structure of the Pyrenean Axial Zone is the result of a polyphased structural evolution related to an oblique continental collision and crustal thickening. Early south-verging thrust sheets involve Silurian to Carboniferous rocks in the hanging wall and Cambro–Ordovician rocks in the footwall (e.g. Bodin & Ledru, 1986; Losantos, Sanz, & Palau, 1986; Majesté-Menjoulas, 1982; Raymond, 1986). The Silurian slates act commonly as the detachment level between the two units. Subsequent south-verging folds and thrusts are related to a widespread regional penetrative cleavage with steep to moderate dips (Carreras & Capella, 1994; Soula, Debat, Déramond, & Pouget, 1986), the so-called D2 phase (Zwart, 1986), which has been characterized as a compressional–transpressional regime with dextral shear motion at the final stages, accompanied by granite intrusions (e.g. Evans, Gleizes,

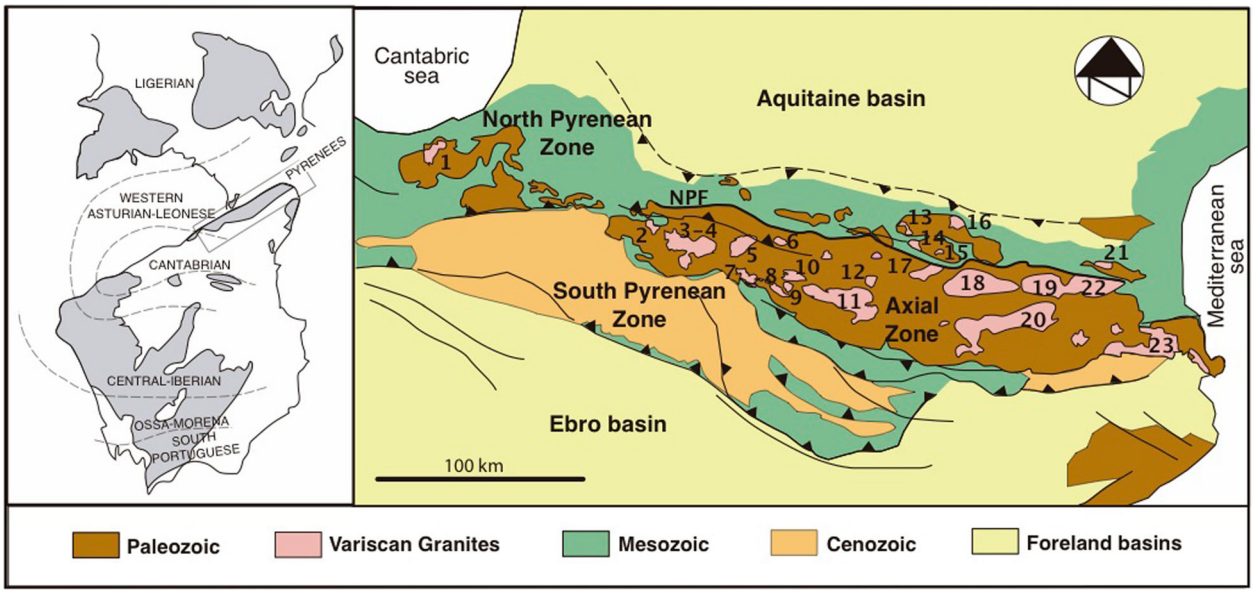

Figure 1. Geological sketch map of the Pyrenees, showing the situation of the Variscan granite bodies from the Axial and North-Pyrenean Zones. 1-Aya, 2-Eaux-Chaudes, 3–4 Cauterets-Panticosa, 5-Néouvielle, 6-Bordères, 7-Bielsa, 8-Millares, 9-Posets, 10-Lys, 11-Maladeta, 12-Marimanha, 13-Lacourt, 14-Ercé, 15-Trois Seigneurs, 16-Foix, 17-Bassiès, 18-Aston Gneiss Dome, 19-Quérigut, 20-Mont-Louis-Andorra, 21-St. Arnac, 22-Millas and 23-St Laurent-La Jonquera.

Leblanc, & Bouchez, 1997; Gleizes, Leblanc, & Bouchez, 1998; Leblanc, Gleizes, Roux, & Bouchez, 1996).

Partial fusion due to crustal thickening during the Variscan orogeny gave rise to calc-alkaline plutonism. The U–Pb ages published in recent decades for the Pyrenean granites indicate that the Variscan plutonism of the Pyrenees is essentially Upper Carboniferous at 301–314 Ma (Denèle, Paquette, Olivier, & Barbey, 2011) and syntectonic (Gleizes, Crevon, Asrat, & Barbey, 2006; Guerrot, 1998, 2001; Maurel, Respaut, Monié, Arnaud, & Brunel, 2004; Olivier, Gleizes, & Paquette, 2004; Paquette, Gleizes, Leblanc, & Bouchez, 1997; Roberts, Pin, Clemens, & Paquette, 2000; Romer & Soler, 1995). A younger plutonism, Permian in age (267 ± 1 Ma) has recently been obtained for the Aya pluton (Denèle et al., 2011). These magmatic bodies are found in low-grade or middle-grade metamorphic domains, following the dominant trend of the Variscan structures. Some authors have claimed coeval development of this magmatism with metamorphism and the main Variscan deformation (e.g. Carreras & Druguet, 1994; Evans, Gleizes, Leblanc, & Bouchez, 1998; Leblanc et al., 1996).

Pioneer studies of AMS in Pyrenean granites focused on the Panticosa, Mont-Louis, Foix, and Posets massifs (Bouchez, Gleizes, Djouadi, & Rochette, 1990; García-Maiztegi, Aranguren, & Tubía, 1991; Gleizes & Bouchez, 1989; Santana & Tubía, 1988). These investigations were led by the Laboratoire des Mécanismes de Transfert en Géologie from the Université Paul-Sabatier – Observatoire Midi Pyrénées (Toulouse), which has tackled 13 batholiths in recent decades. The University of the Basque Country (García-Maiztegi et al., 1991; Hilario, Aranguren, Tubía, & Pinotti, 2003; Santana, Bouchez, Gleizes, & Tubía, 1992) and the University of Zaragoza (Pueyo, Román, Bouchez, Casas, & Larrasoaña, 2004; Román-Berdiel, Casas, Oliva-Urcia, Pueyo, & Rillo, 2004) have continued this research, investigating six additional massifs. Currently, studies on AMS have been completed in 21 plutons, and cover almost all Pyrenean massifs (25). These studies combined have provided evidence of the syntectonic character of the granite bodies, and have allowed a new emplacement model under a dextral transpressive regime to be proposed, related to the D2 Variscan deformation phase (Antolín-Tomás et al., 2009; Auréjac, Gleizes, Diot, & Bouchez, 2004; Evans et al., 1997, 1998; Gleizes, Leblanc, & Bouchez, 1998, Gleizes, Leblanc, Santana, Olivier, & Bouchez, 1998, Gleizes, Leblanc, Olivier, & Bouchez, 2001; Gleizes et al., 2006; Izquierdo-Llavall et al., 2012; Leblanc et al., 1996; Román-Berdiel et al., 2004, 2006). The main structures observed in the granites are magmatic fabrics and localized shear zones with late-Variscan and Alpine ages (Carreras & Cires, 1986; Román-Berdiel et al., 2004).

4. Methodology

The AMS technique is based on the measurement of the magnetic susceptibility (k) of a standard cylindrical sample (25 mm diameter and 22 mm height) in different directions, in order to calculate the magnetic ellipsoid of that sample. This method is based on the relation between the induced magnetization (M) with the magnetic field (H), where $M = kH$. The magnetic susceptibility k is a third-order tensor that can be graphically described by an ellipsoid whose three axes k_1, k_2, and k_3 (also called k_{max}, k_{int}, and k_{min}) correspond to the maximum, intermediate, and minimum susceptibilities, respectively (Figure 2).

Magnetic fabric analysis is a powerful approach for studying granite bodies, because it may provide magmatic information at a regional scale, in rocks where fabrics are difficult to measure optically or by other techniques (Bouchez, 2000). Providing that the paramagnetic content dominates the bulk susceptibility (i.e. biotite and amphibolite are the main carriers) and because of the correspondence between the crystallographic and susceptibility main directions of phyllosilicates (Martín-Hernández & Hirt, 2003) then, a direct comparison between the magmatic and magnetic fabrics can be established. In these cases, the AMS can be interpreted in terms of mineral- (phyllosilicate) preferred orientation; the principal AMS axis ($k1$) is then directly correlated to the magmatic lineation and the minimum axis ($k3$) can be considered as the pole of the magmatic foliation. However, recent studies suggest that during the emplacement (magmatic conditions) some deformation phases may overprint each other contributing to the finite strain ellipsoid and, thus, the study of AMS alone does not necessarily unravel the complete deformational history of the granite (Schulmann & Ježek, 2012). In addition, the correspondence between deformation axes from felspar and biotite is not always univocal (Kratinová et al., 2010; Román-Berdiel, Pueyo-Morer, & Casas-Sainz, 1995). In this sense, some work in weakly deformed sedimentary rocks suggests the importance of magnetic

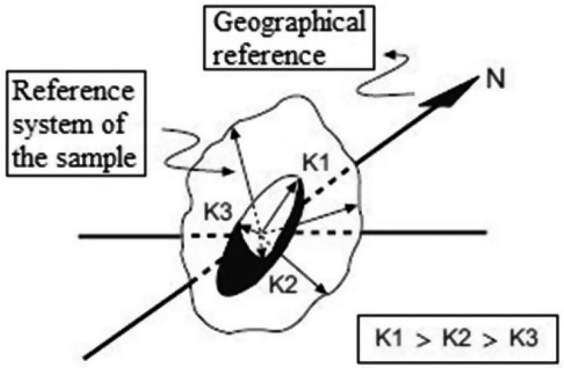

Figure 2. Concept and variable of the AMS ellipsoid (modified from Bouchez, 1997).

subfabric separation (Oliva-Urcia et al., 2009) to disentangle the deformation history. This problem is beyond the scope of this paper and we simply respect the original interpretation of the source papers to build the overview map. Studies of AMS measurements in calc-alkaline granites were pioneer in the Pyrenees (Bouchez et al., 1990; García-Maiztegi et al., 1991; Gleizes & Bouchez, 1989; Santana & Tubía, 1988) and usually assume a simple deformational history during the emplacement; they hypothesized that AMS blocks an infinitesimal deformation ellipsoid coincident with the finite strain tensor.

The variables represented on the maps of this paper are briefly described below; the orientation of the magnetic foliation (plane perpendicular to k_3), lineation (k_1), and the magnetic bulk susceptibility (km). Using the magnitude of the k_1, k_2, and k_3 axes, it is possible to obtain some simple parameters, as the average of the magnetic susceptibility is obtained from:

$$km = (k_1 + k_2 + k_3)/3.$$

5. Sources of data

5.1 Raw data

More than 20 papers and PhD theses from different authors (see Table 1) have been compiled to merge the data necessary to build the synthetic maps. These data also required a homogenization process in order to represent all the variables in the same units and formats. Unfortunately, the raw data from the papers were mostly given in tables and represented on large-scale maps, without the corresponding georeferenced information (Figure 3). In this paper, every map and every measurement site has been georeferenced and all the information has been compiled into new tables.

5.2 Raw maps

Some cartographic resources to construct the maps were used as background layers in the GIS project:

- The two main sources of geologic maps were the Geologic and Mining Spanish Institute (IGME) and the French Geological Survey (BRGM). On one side, the IGME provides the MAGNA maps (1:50,000 scale), on the other, the BRGM also provides the entire French territory at the same scale. As shown in Figure 4, we combine both sources depending on location of the granite (whether it is located in France or in Spain). On the left side, the figure shows two different layers: the Aya pluton shape, laid over the MAGNA map. On the right side, the figure shows Neouvielle pluton drawn on *Google Earth*. MAGNA maps are available online (http://info.igme.es/cartografia/magna50.asp).
- Moreover, there are very few cartographic compilations in the Pyrenees. The recent map by Barnolas et al. (2008) has been used as a background map (Figure 5(a)). However, the simplicity of the structural map of the Pyrenees by Choukroune and Séguret (1973, Figure 5(b)) inspired other authors (Ramón Ortiga, 2013) to modify the Barnolas map. In this paper, we have used the simplified version used by Ramón Ortiga (2013, Figure 5(c)).

Table 1. AMS data from the Pyrenees, sorted by alphabetical order of the granite bodies (modified and enlarged from Pueyo et al., 2006).

	Name (abbreviation in maps)	Sites	Surface (km^2)	Sites/km^2	K bulk (10–6 S.I.)	References
1	Aston Dome (AS)	247	345	0.7	183	Denèle et al. (2009)
2	Aya (AY)	93	57	1.6	174	Olivier, Ameglio, Richen, and Vadeboin (1999)
3	Bassiès (BA)	88	90	1.0	172	Gleizes, Leblanc, and Bouchez (1991)
4	Bielsa (BI)	60	58	1.0	180	Román-Berdiel et al. (2004)
5	Borderes (BO)	64	21	3.0	323	Gleizes et al. (2006)
6–7	Cauterets-Panticosa (CA, PA)	310 (200 + 110)	252 (210 + 42)	1.2	211	Gleizes, Leblanc, Santana, et al. (1998) and Santana (2001)
8	Eaux-Chaudes (EC)	28	19	1.5	304	Izquierdo Llavall (2010) and Izquierdo-Llavall et al. (2012)
9	Ercé (ER)	46	37	1.2	169	Heller (1992)
10	Foix (FO)	69	45	1.5	172	Bouchez et al. (1990)
11	Lacourt (LA)	21	16	1.3	274	Gleizes, Bouchez, Lespinasse, and Roux (1992)
12	Lys (LY)	101	55	1.8	211	Hilario et al. (2003) and Hilario Orús (2004)
13	Maladeta (MA)	253	415	0.6	213	Leblanc, Gleizes, Lespinasse, Olivier, and Bouchez (1994)
14	Marimanha (MH)	62	32	1.9	203	Antolín-Tomás (2006) and Antolín-Tomás et al. (2009)
15	Millares (MI)	54	30	1.8	270	Román-Berdiel et al. (2006)
16	Mont-Louis-Andorra (ML)	254	550	0.5	195	Gleizes (1990) and Gleizes et al. (1993)
17	Néouvielle (NE)	132	104	1.3	220	Gleizes et al. (2001)
18	Posets (PO)	69	21	3.3	270	García-Maiztegi et al. (1991) and Hilario Orús (2004)
19	Quérigut (QU)	121	200	0.6	227	Auréjac et al. (2004)
20	St Laurent – La Jonquera (LJ)	188	298	0.6	212	Olivier, Druguet, Castaño, and Gleizes (2016)
21	St Arnac (ST)	117	30	3.9	303	Olivier, Gleizes, Paquette, and Muñoz-Sáez (2008)
22	Trois Seigneurs (TS)	34	10	3.4	237	Leblanc et al. (1996)
	Total	2157	2340	0.92	231.2	

AMS data for the 28 sampling sites of the Eaux-Chaudes pluton

Site	N	K_1	α95% K_1	K_3	α95% K_3	K_m (10^{-6} SI)	e	Pj	e	T	e
E1	8	030/76	14/07	167/11	27/13	198	83.1	1.068	0.043	−0.170	0.410
E2	9	188/52	26/13	318/27	36/12	153	36.3	1.042	0.018	0.326	0.440
E3	5	214/08	58/42	24/82	68/25	156	20.5	1.057	0.035	0.219	0.233
E4	5	108/26	25/09	311/62	25/20	112	21	1.032	0.009	0.069	0.405
E5	9	193/22	46/15	048/64	19/14	117	23.6	1.025	0.007	0.186	0.292
E6	11	275/03	24/17	177/74	41/10	150	19.1	1.064	0.062	0.148	0.288
E7	11	082/13	49/34	301/73	68/26	97.1	37.6	1.042	0.021	0.269	0.438
E8	12	268/24	26/18	121/62	28/17	158	23.6	1.037	0.015	0.092	0.502
E9	12	304/27	28/17	199/27	64/13	292	56.2	1.035	0.018	0.186	0.393
E10	11	048/17	44/11	181/66	16/11	159	6.99	1.037	0.013	0.144	0.453
E11	10	353/71	76/23	160/19	25/20	199	27.7	1.022	0.009	0.162	0.404
E12	15	294/45	51/23	152/38	73/23	214	20.3	1.026	0.008	0.125	0.317
E13	12	057/04	22/20	325/24	44/22	214	22.6	1.026	0.008	−0.015	0.427
E14	13	053/04	58/38	144/18	53/29	320	72.2	1.035	0.024	0.216	0.409
E15	10	233/07	34/19	086/82	31/17	19.2	5.24	1.066	0.026	0.287	0.462
E16	6	122/10	31/12	281/80	26/11	92.7	21.0	1.035	0.015	0.245	0.441
E17	5	105/13	37/06	342/67	09/07	143	28.6	1.034	0.020	−0.035	0.482
E18	14	116/51	13/05	268/35	14/04	123	12.9	1.059	0.011	0.435	0.229
E19	15	272/31	18/04	054/53	06/06	177	46.5	1.096	0.069	0.287	0.393
E20	7	012/36	21/14	153/47	52/15	257	23.2	1.024	0.008	−0.116	0.205
E21	8	113/76	31/08	349/08	30/20	206	30.5	1.042	0.013	0.128	0.400
E22	11	074/04	24/10	342/28	19/10	41.4	7.54	1.098	0.049	0.648	0.272
E23	7	088/13	38/27	266/77	30/26	171	44.8	1.027	0.010	−0.116	0.466
E24	11	116/68	13/11	003/09	19/09	231	83.7	1.035	0.014	0.023	0.436
E25	15	280/12	30/24	141/74	36/24	110	18.5	1.030	0.008	0.152	0.276
E26	9	151/15	32/24	012/71	72/24	105	12.1	1.033	0.011	0.168	0.445
E27	11	047/12	32/16	212/78	27/13	121	18.9	1.025	0.010	0.105	0.385
E28	16	266/09	34/11	093/81	12/11	136	27.5	1.035	0.008	0.375	0.345

N, number of specimens. K_1 and K_3, mean (trend/plunge) of the magnetic lineation and of the pole of the magnetic foliation (Jelinek 1977); α95, maximum and minimum angles for the confidence ellipse with the 95% probability (Jelinek 1977); K_m, magnitude of the magnetic susceptibility (in 10^{-6} S.I.); Pj, corrected anisotropy degree (Jelinek 1981); *T*, shape parameter (Jelinek 1981); *e*, standard error

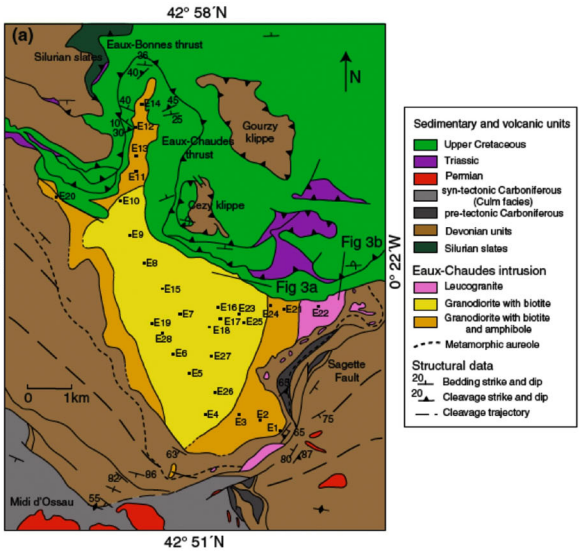

Figure 3. Example of AMS data from the paper by Izquierdo-Llavall et al. (2012) in the Eaux-Chaudes massif in the westernmost part of the Axial Zone. Left: table of raw data displaying standard information. Right: geological map. This was the only case in which the authors provided the original UTM coordinates of the sites taken in the field with a GPS. In the remaining cases, we had to extract the geo-positioning using this kind of graphic information.

6. Discussion

6.1 Georeferencing errors

The original maps that were contained in the papers had very poor geographic information (both quality and accuracy). This fact made the geo-positioning process difficult, and errors could not be fully avoided. The following table shows the mean errors found in each granite. No quantifiable units (e.g meters) are given for the errors because the original maps (extracted from the papers) do not supply such information (Table 2).

6.2 Standardization of information

In this paper, when discussing AMS spherical information, we had to face three main problems: (1) data were represented in scalar format, thus they had to be converted to directional format with hundreds of measurements; (2) in some cases magnetic foliation had to be converted into k_3; (3) most of the direction data needed to be changed into stereographic space (360°) instead of the 180° space used by some authors, which meant adding the N–S–E–W. This last step was of vital importance because, although the reader may easily understand that 210° = 30S, the software *ArcGIS* is unable to do so.

6.3 Global data information

In total, 21 different tables (one for each granitic body) with about 2210 sites and more than 12,000 different data were obtained. These results have been synthesized in three different maps:

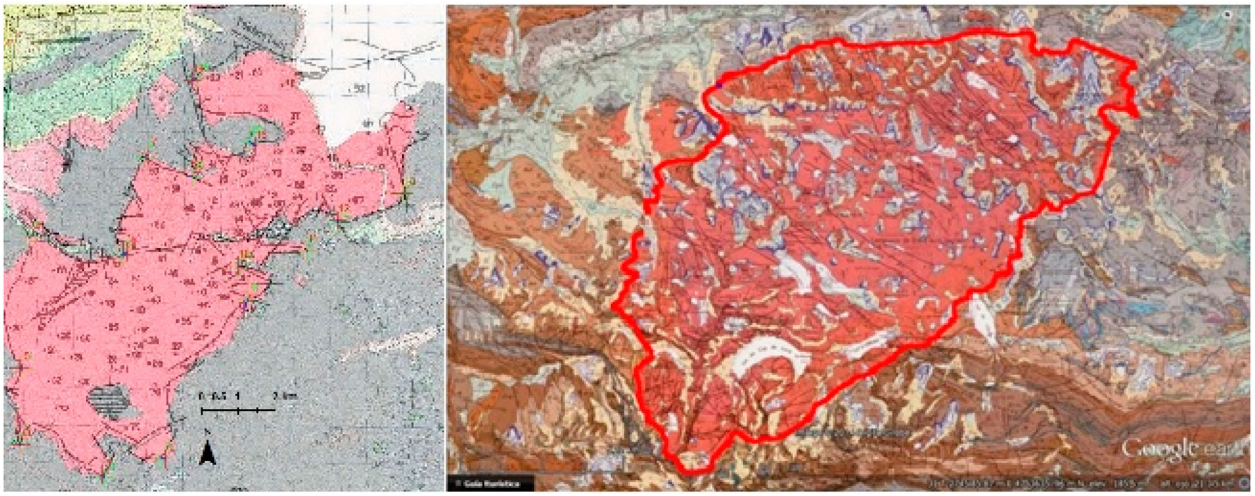

Figure 4. Example of MAGNA (left) and BRGM (on Google Earth, right) maps for the Aya and Neouvielle Plutons. The contact with the host rocks has been highlighted and used as a main marker during the georeferencing process.

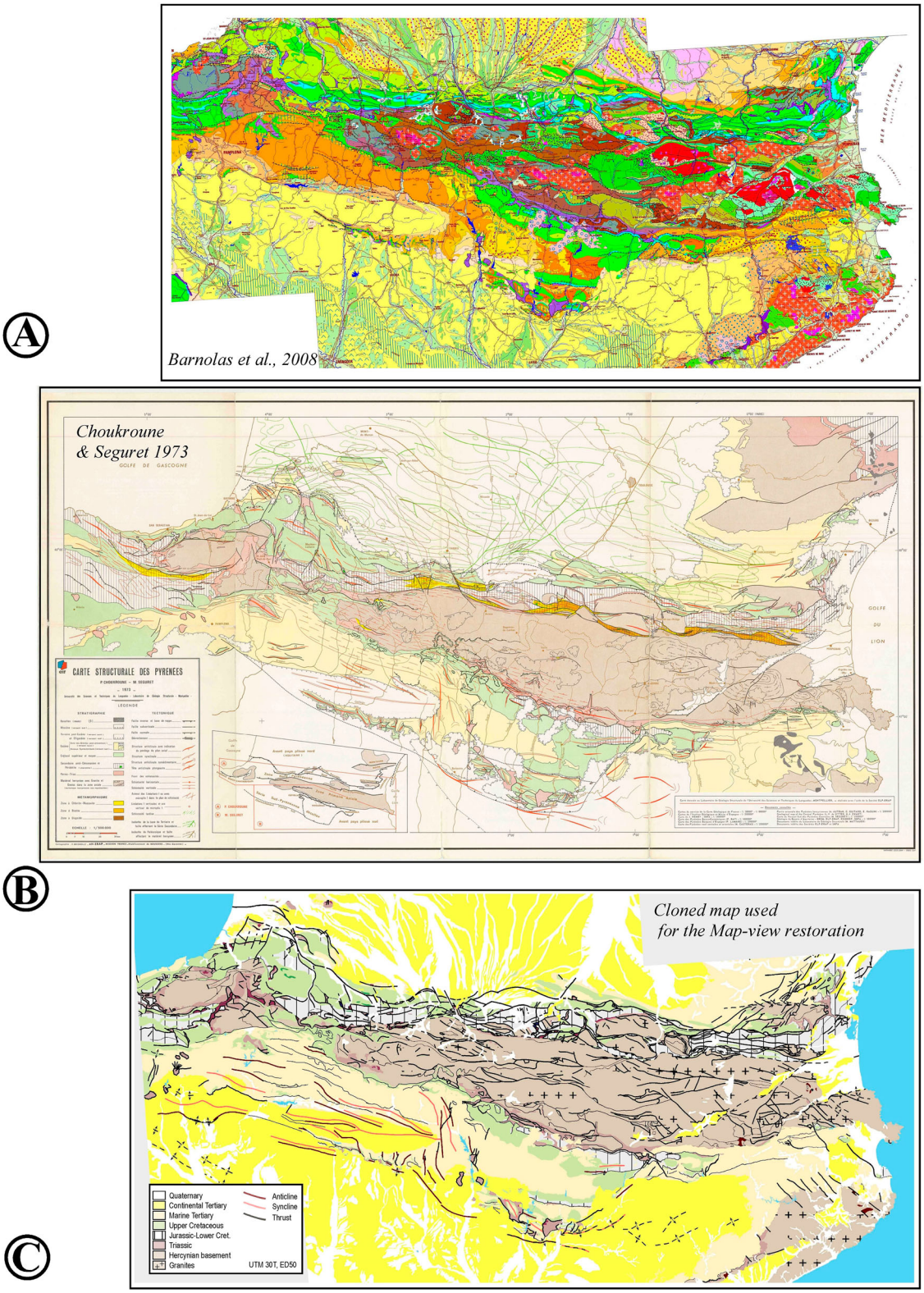

Figure 5. The addition of (A) the map by Barnolas et al. (2008) plus (B) the style and simplicity of the map by Choukroune and Séguret (1973) has given rise to (C) our background map. Taken from (Ramón Ortiga, 2013).

The *bulk susceptibility map* contains site mean values and a mapping following fixed intervals of susceptibility for all bodies. This information allows us to rapidly assess the total iron distribution in the Pyrenean plutons, and therefore an approach to the petrologic facies. These intervals have been set according to Gleizes et al. (1993), who proposes a correspondence between bulk susceptibility and petrologic facies. Here, measures below 100×10^{-6} SI correspond to leucogranites; measures from 100 to 200×10^{-6} SI correspond to monzogranites; measures from 201 to 300×10^{-6} SI correspond to granodiorites; and measures above 300×10^{-6} SI correspond to quartz diorites.

Table 2. Relationship between the number of benchmarks and the error obtained (no defined units) for each granite.

Name	Total benchmarks	Error	Name	Total benchmarks	Error
Aston Gneiss Dome	9	3.5195	Lys	10	3.7007
Aya	15	4.8668	Maladeta	10	3.5116
Bassiès	11	3.6300	Marimanha	7	2.0254
Bielsa	10	2.2151	Millares	10	1.065
Bordères	10	4.1508	Mont-Louis-Andorra	10	3.5666
Cauterets-Panticosa	8	2.0196	Néouvielle	8	0.9016
Eaux Chaudes	10	0.7687	Posets	8	3.1023
Ercé	10	1.6677	Quérigut	10	4.6654
Foix	10	3.7587	St Arnac	14	4.3911
Lacourt	10	4.7548	Trois Seigneurs	9	3.5431

Note: Cauterets–Panticosa was georeferenced as one body.

Interestingly, and apart from the data of the Aston gneissic dome (Denèle, Olivier, Gleizes, & Barbey, 2009), the magnetic susceptibility histogram (Figure 6(right)) displays values similar to those found in many sedimentary rocks (see data from the cover rocks by Pocovi et al., 2014). This robust observation (>10,000 individual measurements) contradicts the general assumption on the magnetic nature of the hercynian basement that has been used in many petrophysical and geophysical studies.

The *Foliation map* includes the magnetic foliation at every site, that is, the plane perpendicular to the k_3 (k_{min}) axis. As there is no deformation in the solid state, it is not possible to comment on pole of the cleavage, but it is true that the pole of k_3 and this pole of cleavage are very similar, which means that granites could have suffered this deformation in a passive way. It is worth noting that only raw data have been plotted, and we have not performed any kind of interpolation. Additionally, we have plotted together in the stereoplot (Cardozo & Allmendinger, 2013; Allmendinger, Cardozo, & Fisher, 2013) all mean data of k_3 orientation (Figure 7, right). Here some observations can be made:

- Although the stereoplot looks slightly noisy, as many peculiarities from every pluton are assembled together, the main eigenvector fitted by Bingham statistics (1974) surprisingly resembles the pole of the Pyrenean cleavage (Choukroune & Séguret, 1973). This fact likely reflects, at least partially, a northward tilt in the plutons caused by alpine basement nappes. Bimodal subhorizontal distributions indicate that most of the bodies are batholites.
- As expected, the main girdle is not coaxial to the present Pyrenean trending.

The *Lineation map* includes the mapping of individual magnetic lineations k_1 (k_{max}) axis. Regarding the overview stereonet, we can highlight some facts:

- Magnetic lineation seems to display a bimodal distribution; ENE–WSW and E–W (Figure 7, left).
- Similar to the possible reworking caused by the alpine tilting detected in the magnetic foliation, the lineations can be fitted to a girdle that could be produced by Pyrenean deformation (passive movement into the basement nappes).

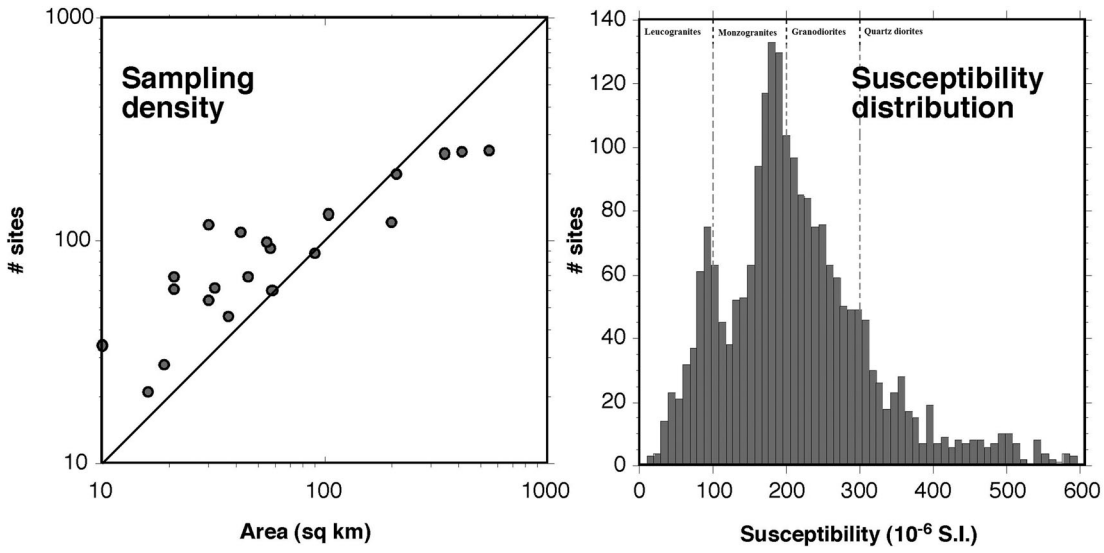

Figure 6. Susceptibility overview. Left: density of sampling of AMS sites per pluton. Larger bodies have a slightly lower density of sampling. Right: Susceptibility distribution following the same classification as on the map, and its correspondence with petrologic facies according to Gleizes et al. (1993). Only site means were considered in this graph. The Aston dome was not considered in these graphs.

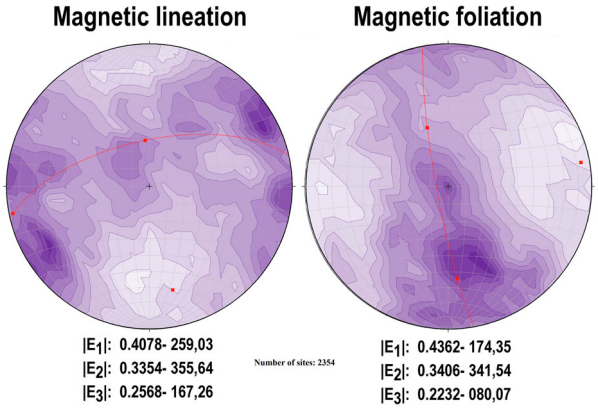

Figure 7. AMS overview. Magnetic lineation (k_1) and pole to magnetic foliation (k_3) stereoplots. Again, only site means were considered. Significance level: 4, contour interval: 2. Eigenventors are also displayed for both modulus and orientation (trend, plunge). *N* is the number of AMS sites considered. Every dot in the stereonet is the mean of a site (3–8 individual measurements). Number of sites considered: 2354.

Regarding the map overviews, both lineation and foliation symbols on the maps have been reproduced following the style used by Román-Berdiel et al. (2004), which is simple and easy to read. In the lineation case, the top of the arrow indicates the direction, and there are three different levels depending on the azimuth results: less than 30°, between 30 and 60°, and more than 60°. For the foliation, there are again three levels to display the dip in each case. In the bulk susceptibility case, we pick a simple green scale following 100 10^{-6} S.I. steps, allowing for quick data interpretation.

7. Conclusions

In this paper, we have synthesized in three different maps the information derived from more than 25 papers and PhD theses on the anisotropy of the magnetic susceptibility of 21 granitic bodies, and one gneissic dome from the Pyrenees. The homogenous cartographic data, together with the standardized magnetic information, allow us to display a better characterization of the regional distribution of the variables; bulk susceptibility (*k*m), magnetic lineation (k_1) and pole to magnetic foliation (k_3).

Specifically, 22 bodies (21 granites and a gneissic dome) have been redrawn, involving more than 2200 sites with more than 12,000 original AMS measurements. This information is now in a database which we plan to upload on the webGIS servers of the IGME and BRGM (Spanish and French geological surveys). This paper shows only the three final maps for the entire Pyrenees – however, 22 different maps were generated, one for each granite, with their respective table of information.

Software

Esri ArcGIS 10.2 was used for (1) gathering and visualizating the underlying data, (2) georeferencing granite bodies and sites, (3) digitizing and editing magnetic data layers and (4) producing the map layout and corresponding legend.

Disclosure statement

No potential conflict of interest was reported by the authors.

Funding

This work was founded by the projects DR3AM (CGL2014–55118), PmagIGME and GeoPyrDatabases (PI165/09) financed by the MINECO, IGME and the Aragonian Government, respectively.

ORCID

Manuel Porquet http://orcid.org/0000-0002-5127-0153

References

Allmendinger, R. W., Cardozo, N. C., & Fisher, D. (2013). *Structural geology algorithms: Vectors & tensors*: Cambridge: Cambridge University Press. 289 pp.

Antolín-Tomás, B. (2006). Estudio estructural del plutón de Marimanha (Pirineo central). Posgrado de Iniciación a la Investigación en Geología. Universidad de Zaragoza, 128 pp.

Antolín-Tomás, B., Román-Berdiel, T., Casas-Sainz, A., Gil-Peña, I., Oliva, B., & Soto, R. (2009). Structural and magnetic fabric study of the Marimanha granite (axial zone of the Pyrenees). *International Journal of Earth Sciences*, *98*(2), 427–441.

Auréjac, J.-B., Gleizes, G., Diot, H., & Bouchez, J. L. (2004). Le complexe granitique de Quérigut (Pyrénées, France) ré-examiné par la technique de l'ASM: un pluton syntectonique de la transpression dextre hercynienne. *Bulletin de la Société Géologique de France*, *175*(2), 157–174.

Barnolas, A., Gil-Peña, I., Alfageme, S., Ternet, Y., Baudin, T., & Laumonier, B. (2008). Mapa geológico de los Pirineos a escala 1:400 000. IGME/BRGM ISBN: 978-2-7159-2168-9.

Beamud, E., Muñoz, J. A., Fitzgerald, P. G., Baldwin, S. L., Garcés, M., Cabrera, L., & Metcalf, J. R. (2011). Magnetostratigraphy and detrital apatite fission track thermochronology in syntectonic conglomerates: Constraints on the exhumation of the south-central Pyrenees. *Basin Research*, *23*(3), 309–331.

Bingham, C. (1974). An antipodally symmetric distribution on the sphere. *Annals of Statistics*, *2*, 1201–1225.

Bodin, J., & Ledru, P. (1986). Nappes hercyniennes précoces à matériel dévonien hétéropique dans les Pyrénées ariégeoises. *CRAS Paris 302*, *2*(15), 969–974.

Borradaile, G. J., & Henry, B. (1997). Tectonic applications of magnetic susceptibility and its anisotropy. *Earth-Science Reviews*, *42*(1–2), 49–93.

Bouchez, J. L. (1997). Granite is never isotropic: An introduction to AMS studies of granitic rocks (pp. 95–112). Netherlands: Springer.

Bouchez, J. (2000). Magnetic susceptibility anisotropy and fabrics in granites. *Comptes Rendus de l'Académie des Sciences Series IIA Earth and Planetary Science*, *330*(1), 1–14.

Bouchez, J. L., Gleizes, G., Djouadi, T., & Rochette, P. (1990). Microstructure and magnetic susceptibility applied to emplacement kinematics of granites: The example of the Foix pluton (French Pyrenees). *Tectonophysics*, *184*(2), 157–171.

Cardozo, N., & Allmendinger, R. W. (2013). Spherical projections with OSXStereonet. *Computers & Geosciences*, *51*(0), 193–205. 10.1016/j.cageo.2012.07.021.

Carreras, J., & Capella, I. (1994). Tectonic levels in the Paleozoic basement of the Pyrenees: A review and a new interpretation. *Journal of Structural Geology*, *16*, 1509–1524.

Carreras, J., & Cires, J. (1986). The geological significance of the western termination of the Merens fault at Port Vell (central Pyrenees). *Tectonophysics*, *129*, 99–114.

Carreras, J., & Druguet, E. (1994). Structural zonation as a result of inhomogeneous non-coaxial deformation and its control on syntectonic intrusions: An example from the Cap de Creus area; eastern Pyrenees. *Journal of Structural Geology*, *2*, 5–9.

Choukroune, P., & Séguret, M. (1973). Carte structurale des Pyrénées, 1/500.000, Université de Montpellier – ELF Aquitaine.

Denèle, Y., Olivier, P., Gleizes, G., & Barbey, P. (2009). Decoupling between the middle and upper crust during transpression-related lateral flow: Variscan evolution of the Aston gneiss dome (Pyrenees, France). *Tectonophyisics*, *477*, 244–261.

Denèle, Y., Paquette, J. L., Olivier, P., & Barbey, P. (2011). Permian granites in the Pyrenees: The Aya pluton (Basque country). *Terra Nova*, *00*, 1–9.

Ellwood, B. B., & Wenner, D. B. (1981). Correlation of magnetic susceptibility and oxygen isotopic values in late orogenic granites of the southern Appalachian piedmont. *Earth and Planetary Science Letters*, *54*, 200–202.

Evans, N. G., Gleizes, G., Leblanc, D., & Bouchez, J. L. (1997). A new interpretation of the Hercynian tectonics in the Pyrenees based on the detailed examination of structures around the Bassies granite. *Journal of Structural Geology*, *19*, 195–208.

Evans, N. G., Gleizes, G., Leblanc, D., & Bouchez, J. L. (1998). Syntectonic emplacement of the Maladeta granite (Pyrenees) deduced from relationships between Hercynian deformation and contact metamorphism. *Geological Society of Londons*, *155*, 209–216.

Fitzgerald, P. G., Muñoz, J. A., Coney, P. J., & Baldwin, S. L. (1999). Asymmetric exhumation across the Pyrenean orogen: Implications for the tectonic evolution of a collisional orogen. *Earth and Planetary Science Letters*, *173*(3), 157–170.

García-Maiztegi, C., Aranguren, A., & Tubía, J. M. (1991). Zonación magnética y caracterización del elipsoide de la susceptibilidad magnética en el plutón de Posets (Pirineos Centrales). *Geogaceta*, *10*, 138–140.

Gleizes, G. (1990). Structure des granites hercyniens des Pyrénées de Mont Louis-Andorre a la Maladeta (Thèse de doctorat). Université de Toulouse III.

Gleizes, G., & Bouchez, J. L. (1989). Le granite de Mont-Louis (Zone axiale des Pyrénées): anisotropie magnétique, structures et microstructures. *Comptes Rendus de l'Académie des Sciences Paris*, *309*(II), 1075–1082.

Gleizes, G., Bouchez, J. L., Lespinasse, P., & Roux, L. (1992). Structure du granite de Lacourt (Arize occidentale): une signature syntectonique de phase 2 dans l'Hercynien des Pyrénées. *Bulletin de la Société d'histoire naturelle de Toulouse*, *128*, 53–57.

Gleizes, G., Crevon, G., Asrat, A., & Barbey, P. (2006). Structure, age and mode of emplacement of the Hercynian Bordères-Louron pluton (central Pyrenees, France). *The International Journal of Earth Sciences*, *95*, 1039–1052.

Gleizes, G., Leblanc, D., & Bouchez, J. L. (1991). Le pluton granitique de Bassiès (Pyrénées ariégeoises): zonation, structure et mise en place. *Journal of Geophysical Research, 312*(7), 755–762.

Gleizes, G., Leblanc, D., & Bouchez, J. L. (1998). The main phase of the Hercynian orogeny in the Pyrenees is a dextral transpression. *Journal of Geological society*, *135*(1), 267–273.

Gleizes, G., Leblanc, D., Olivier, P., & Bouchez, J. L. (2001). Strain partitioning in a pluton during emplacement in transpressional regime: The example of the Néouvielle granite (Pyrenees). *International Journal of Earth Sciences*, *90*, 325–340.

Gleizes, G., Leblanc, D., Santana, V., Olivier, P., & Bouchez, J. L. (1998). Sigmoidal structures featuring dextral shear during emplacement of the Hercynian granite complex of Cauterets-Panticosa (Pyrenees). *Journal of Structural Geology*, *20*, 1229–1245.

Gleizes, G., Nédélec, A., Bouchez, J.-L., Autran, A., & Rochette, P. (1993). Magnetic susceptibility of the Mont Louis-Andorra ilmenite-type granite (Pyrenees): A new tool for the petrographic characterization and regional mapping of zoned granite plutons. *Journal of Geophysical Research*, *98*, 4317–4331.

Graham, J. W. (1954). Magnetic susceptibility anisotropy, an unexploited petrofabric element. *Geological Society of America Bulletin*, *65*, 1257–1258.

Guerrot, C. (1998). Résultats de datation U-Pb par dissolution sur zircons pour le granite de Cauterets, Pyrénées. Rapport inédit, SMN/PEA/ISO 146/98 CG/NB, BRGM. In C. Majesté-Menjoulas, F. Debon, & P. Barrère (Eds.), *Notice explicative, carte géol. France* (*1/50 000*), *feuille Gavarnie* (*1082*) (pp. 4). Orléans: BRGM.

Guerrot, C. (2001). Datation du pluton des Eaux-Chaudes. In Y Ternet, C Majesté- Menjoulas, J Canérot, T Baudin, A Cocherie, C Guerrot, & P Rossi (Eds.), (*2004*) *notice explicative, carte géol. France (1/50,000), feuille Laruns-Somport* (*1069*) (pp. 185–187). Orléans: BRGM.

Heller, F. (1973). Magnetic anisotropy of granitic rocks of the Bergell massif (Switzerland). *Earth and Planetary Science Letters*, *20*, 180–188.

Hilario, A., Aranguren, A., Tubía, J. M., & Pinotti, L. (2003). Estructura del plutón sincinemático de Lys (Zona Axial del Pirineo). *Geogaceta*, *34*, 51–54.

Hilario Orús, A. (2004). Relación entre magmatismo y deformación en la transversal de Benasque a Luchon (Zona Axial del Pirineo) (Tesis Doctoral). Universidad del País Vasco UPV/EHU, 300 p.

Ishihara, S. (1977). The magnetite-series and ilmenite-series granitic rocks. *Mining Geology*, *27*, 293–305.

Izquierdo-Llavall, E. (2010). Estudio de la fábrica magnética de Eaux-Chaudes. Relación con la estructura varisca del Pirineo Axial (Trabajo Fin de Master). Universidad de Granada, 130 pp.

Izquierdo-Llavall, E., Román-Berdiel, T., Casas, A. M., Oliva-Urcia, B., Gil-Peña, I., Soto, R., & Jabaloy, A. (2012). Magnetic and structural study of the Eaux-Chaudes intrusion: Understanding the Variscan deformation in the western axial zone (Pyrenees). *International Journal of Earth Sciences*, *101*(7), 1817–1834.

King, R. F. (1966). The magnetic fabric of some Irish granites. *Geological Journal*, *5*, 43–66.

Kratinová, Z., Ježek, J., Schulmann, K., Hrouda, F., Shail, R. K., & Lexa, O. (2010). Noncoaxial K-feldspar and AMS subfabrics in the land's End granite, Cornwall: Evidence of magmatic fabric decoupling during late deformation and matrix crystallization. *Journal of Geophysical Research: Solid Earth*, *115*(B9), 104–125.

Leblanc, D., Gleizes, G., Lespinasse, P., Olivier, P., & Bouchez, J. L. (1994). The Maladeta granite polydiapir, spanish Pyrenees: A detailed magneto-structural study. *Journal of Structural Geology*, *16*, 223–235.

Leblanc, D., Gleizes, G., Roux, L., & Bouchez, J. L. (1996). Variscan dextral transpression in the French Pyrenees: New data from the Pic des Trois-Seigneurs Granodiorite and its country rocks. *Tectonophysics*, *261*, 331–345.

López, M. A., Oliván, C., Oliva, B., Pueyo, E. L. and the GeoKin3DPyr working, (2008). Pyrenean paleomagnetic databases. *Geotemas*, 10, 1219–1222.

Losantos, M., Sanz, J., & Palau, J. (1986). Considerations about hercynian thrusting in the Marimanya massif (central Pyrenees). *Tectonophysics*, *129*, 71–79.

Majesté-Menjoulas, C. (1982). L'unité paléozoïque de Bachebirou-Chinipro, témoin d'une tectonique tangencielle varisque dans les Pyrénées Centrales. *CRAS*, *294* (2), 145–150.

Martín-Hernández, F., & Hirt, A. M. (2003). The anisotropy of magnetic susceptibility in biotite, muscovite and chlorite single crystals. *Tectonophysics*, *367*(1), 13–28.

Maurel, O., Respaut, J. P., Monié, P., Arnaud, N., & Brunel, M. (2004). U-Pb emplacement and 40Ar/39Ar cooling ages of the Mont-Louis granite massif (eastern Pyrenees, France). *C. R. Geosci.*, *336*, 1091–1098.

Muñoz, J.A. (1992). Evolution of a continental collision belt: ECORS-Pyrenees crustal balanced cross-section. In: K.R. McClay (Ed.), *Thrust tectonic* (pp. 235–246). Dordrecht: Springer Netherlands.

Oliva-Urcia, B., Larrasoaña, J. C., Pueyo, E. L., Gil, A., Mata, P., Parés, J. M., & Pueyo, O. (2009). Disentangling magnetic subfabrics and their link to deformation processes in cleaved sedimentary rocks from the internal sierras (west central Pyrenees, Spain). *Journal of Structural Geology*, *31*(2), 163–176.

Olivier, P., Ameglio, L., Richen, H., & Vadeboin, F. (1999). Emplacement of the Aya Variscan granitic pluton (Basque Pyrenees) in a dextral transcurrent regime inferred from a combined magnetostructural and gravimetric study. *Journal of the Geological Society*, *156*, 991–1002.

Olivier, P., Druguet, E., Castaño, L. M., & Gleizes, G. (2016). Granitoid emplacement by multiple sheeting during Variscan dextral transpression: The Saint-Laurent–La Jonquera pluton (eastern Pyrenees). *Journal of Structural Geology*, *82*, 80–92.

Olivier, P., Gleizes, G., & Paquette, J. L. (2004). Gneiss domes and granite emplacement in an obliquely convergent regime: New interpretation of the Variscan Agly Massif (Eastern Pyrenees, France). *Geological Society of America Special Papers*, *380*, 229–242.

Olivier, P., Gleizes, G., Paquette, J. L., & Muñoz-Sáez, C. (2008). Structure and U-Pb dating of the Saint Arnac pluton and the Ansignan Charnockite (Agly massif): A cross section from the upper to the middle crust of the Variscan eastern Pyrenees. *Journal of the Geological Society*, *165*, 141–152.

Paquette, J. L., Gleizes, G., Leblanc, D., & Bouchez, J. L. (1997). Le granite de Bassiès (Pyrénées): un pluton syntectonique d'âge Westphalien. Géochronologie U-Pb sur zircons. *CRAS Paris*, *324*, 387–392.

Parés, J. M. (2015). Sixty years of anisotropy of magnetic susceptibility in deformed sedimentary rocks. *Frontiers in Earth Science*, *3*(4), 1–13.

Pocovi, A., Pueyo Anchuela, Ó, Pueyo, E. L., Casas-Sainz, A. M., Román Berdiel, M. T., Gil Imaz, A., Villalaín, J. J. (2014). Magnetic fabrics in the central-western Pyrenees: An overview. In B. Almqvist, B. Henry, M. Jackson, T. Werner, & F. Lagroix (Eds.), *ASM in deformed rocks a tribute to Graham J. Borradaile* (pp. 303–318). Zaragoza, Spain: Tectonophysics. 629.

Porquet, M. (2014). Sistema de Información Geográfica de las propiedades magnéticas de los granitos del Pirineo (MSc thesis). Universidad de Zaragoza. 128 pp. http://zaguan.unizar.es/record/31132.

Pueyo, E. L., López, M. A., Bouchez, J. L., Román, M. T., Cuevas, J., Antolín, B., Navas, J. (2006). *The Pyrenean AMS database, state of the art and future tasks.* Proceedings of Geokin3Dpyr, (2006), 6 pp.

Pueyo, E. L., Román, M. T, Bouchez, J. L, Casas, A. M., .Larrasoaña, J. C. (2004). Statistical significance of magnetic fabric data in studies of paramagnetic granites. In: F. Martín-Hernández, C. M. Lüneburg, C. Aubourg, & M. Jackson, (Eds.), *Magnetic fabric: Methods and applications* (pp. 395–420). Geological Society of London Special Publication. doi: 0.1144/ GSL.SP.2004.238.01.21

Ramón Ortiga, M. J. (2013). Flexural unfolding of complex geometries in fold and thrust belts using paleomagnetic vectors (Unpublished PhD). University of Zaragoza, 228 pp.

Raymond, D. (1986). Tectonique tangentielle varisque dans le Paléozoique supérieur de l'Est des Pyrénées françaises; l'exemple du Pays de Sault (Nord du granite de Quérigut, Aude et Ariège) et des régions voisines.
Bulletin de la Société Géologique de France, *2*(*3*), 479–485.

Roberts, M. P., Pin, C., Clemens, J. D., & Paquette, J. L. (2000). Petrogenesis of Mafic to Felsic plutonic rock associations: The calc-alkaline Quérigut complex, French Pyrenees. *Journal of Petrology*, *41*(6), 809–844.

Román-Berdiel, T., Casas, A., Oliva-Urcia, B., Pueyo, E. L., Liesa, C., & Soto, R. (2006). The Variscan Millares granite (central Pyrenees): Pluton emplacement in a T fracture of a dextral shear zone. *Geodinamica Acta*, *19*, 197–211.

Román-Berdiel, T., Casas, A., Oliva-Urcia, B., Pueyo, E. L., & Rillo, C. (2004). The main Variscan deformation event in the Pyrenees: New data from the structural study of the Bielsa granite. *Journal of Structural Geology*, *26*(2004), 654–677.

Román-Berdiel, T., Pueyo-Morer, E. L., & Casas-Sainz, A. M. (1995). Granite emplacement during contemporary shortening and normal faulting: Structural and magnetic study of the Veiga massif (NW Spain). *Journal of Structual Geology*, *17*, 1689–1706.

Romer, R. L., & Soler, A. (1995). U-Pb age and lead isotopic characterization of Au-bearing Skarn related to the Andorra granite (central Pyrenees, Spain*). Mineralium Deposita*, *30*, 374–383.

Santana, V. (2001). El plutón de Panticosa (Huesca, Pirineos): Estructura y modelo de emplazamiento a partir del análisis de la anisotropía de la susceptibilidad magnética. Tesis Doctoral, Universidad del País Vasco UPV/EHU, 146 p. & 7 anexos.

Santana, V., Bouchez, J. L., Gleizes, G., & Tubía, J. M. (1992). En: III Congreso Geológico de España. *Comunicaciones*, *2*, 179–185.

Santana, V., & Tubía, J. M. (1988). Análisis de la estructura del macizo granítico de Panticosa: Datos preliminares. Symposium on the geology of the Pyrenees and Betics. Barcelona, p. 54.

Schulmann, K., & Ježek, J. (2012). Some remarks on fabric overprints and constrictional AMS fabrics in igneous rocks. *International Journal of Earth Sciences*, *101*(3), 705–714.

Soula, J. C., Debat, P., Déramond, J., & Pouget, P. (1986). A dynamic model of the structural evolution of the Hercynian Pyrenees. *Tectonophysics*, *129*, 29–51.

Tarling, D. H., & Hrouda, F. (1993). *The magnetic anisotropy of rocks*. London: Chapman & Hall, 217 p.

Vera, J. A. (editor) (2004). *Geología de españa*. Madrid: SGE-IGME.

Zwart, H. J. (1986). The Variscan geology of the Pyrenees. *Tectonophysics*, *129*, 9–27.